THE JOURNAL OF BIOLOGICAL CHEMISTRY VOL. 288, NO. 19, pp. 13258–13268, May 10, 2013

The Auxiliary Subunit KChIP2 Is an Essential Regulator of Homeostatic Excitability*

Received for publication, November 7, 2012, and in revised form, March 22, 2013 Published, JBC Papers in Press, March 27, 2013, DOI 10.1074/jbc.M112.434548

Hong-Gang Wang[‡§], Xiao Ping He[¶], Qiang Li[‖‡‡], Roger D. Madison[¶**‡‡], Scott D. Moore[¶‖‡‡], James O. McNamara[¶], and Geoffrey S. Pitt[‡§¶1]**

*From the [‡]Division of Cardiology, Department of Medicine, the [§]Ion Channel Research Unit, and the Departments of [¶]Neurobiology, [‖]Psychiatry, and **Neurosurgery, Duke University, Medical Center, Durham, North Carolina 27710 and the [‡‡]Durham Veterans Affairs Medical Center, Durham, North Carolina 27710*

Background: The necessity for, or redundancy of, distinctive KChIP proteins is not known.
Results: Deletion of KChIP2 leads to increased susceptibility to epilepsy and to a reduction in I_A and increased excitability in pyramidal hippocampal neurons.
Conclusion: KChIP2 is essential for homeostasis in hippocampal neurons.
Significance: Mutations in K^+ channel auxiliary subunits may be loci for epilepsy.

The somatodendritic I_A (A-type) K^+ current underlies neuronal excitability, and loss of I_A has been associated with the development of epilepsy. Whether any one of the four auxiliary potassium channel interacting proteins (KChIPs), KChIP1–KChIP4, in specific neuronal populations is critical for I_A is not known. Here we show that KChIP2, which is abundantly expressed in hippocampal pyramidal cells, is essential for I_A regulation in hippocampal neurons and that deletion of *Kchip2* affects susceptibility to limbic seizures. The specific effects of *Kchip2* deletion on I_A recorded from isolated hippocampal pyramidal neurons were a reduction in amplitude and shift in the $V_{½}$ for steady-state inactivation to hyperpolarized potentials when compared with WT neurons. Consistent with the relative loss of I_A, hippocampal neurons from *Kchip2*$^{-/-}$ mice showed increased excitability. WT cultured neurons fired only occasional single action potentials, but the average spontaneous firing rate (spikes/s) was almost 10-fold greater in *Kchip2*$^{-/-}$ neurons. In slice preparations, spontaneous firing was detected in CA1 pyramidal neurons from *Kchip2*$^{-/-}$ mice but not from WT. Additionally, when seizures were induced by kindling, the number of stimulations required to evoke an initial class 4 or 5 seizure was decreased, and the average duration of electrographic seizures was longer in *Kchip2*$^{-/-}$ mice compared with WT controls. Together, these data demonstrate that the KChIP2 is essential for physiologic I_A modulation and homeostatic stability and that there is a lack of functional redundancy among the different KChIPs in hippocampal neurons.

The potassium channel interacting proteins (KChIPs 1–4)[2] are a subfamily of neuronal calcium sensor proteins that were originally identified as partners for Kv4 α subunits in a yeast two-hybrid screen (1, 2). Through these interactions, KChIPs modulate trafficking, targeting to the plasma membrane, as well as turnover and endocytosis of Kv4 channels. Co-expression of Kv4 α subunits with one of the KChIPs results in larger currents that inactivate more slowly and recover from inactivation more quickly than the currents generated by Kv α-subunits expressed alone (1). All four KChIPs are expressed in brain (1, 2).

Kv4 α subunits, the major targets of KChIP2, are pore-forming subunits of the neuronal somatodendritic A-type K current (I_A). I_A regulates neuronal activity mainly through effects on excitatory postsynaptic potentials and back-propagated action potentials (3, 4). By severely dampening dendritic excitability, I_A influences dendritic integration and propagation of information and modulates the input and output relationship of electrical signals. Reductions in the Kv4.2 channel mRNA or protein level have been demonstrated in animal models of epilepsy (5–8). A mutation in *KCND2*, the gene encoding Kv4.2, was found in a patient with temporal lobe epilepsy (9).

Whether any one KChIP plays a distinctive and essential role in I_A regulation or whether there is functional redundancy among the KChIPs is not known. Knock-out of KChIP2 or KChIP3 is associated with compensatory up-regulation of other KChIPs in posterior cortical neurons. I_A density was unaffected by KChIP2 knock-out but mildly reduced by KChIP3 knock-out regardless of the expression levels of other KChIPs (10). This suggests that KChIP3 may have a more prominent role in posterior neurons. Distinctive roles in I_A regulation for individual KChIPs in other areas have not been tested, however, and not all neurons may be capable of the same compensatory changes present in posterior cortical neurons. Specifically, whether the absence of KChIP2 affects function of neurons outside of the posterior cortex or has physiological effects has not been reported.

Here, we investigated the role of KChIP2 in hippocampal neurons and in epilepsy. We focused specifically on hippocam-

* This work was supported, in whole or in part, by National Institutes of Health Grants R01 HL71165 and R01 HL088089 (to G. S. P.) and R01NS056217 (to J. O. M.). This work was also supported by grant from Citizens United for Research in Epilepsy (to G. S. P.).

[1] To whom correspondence should be addressed: Ion Channel Research Unit, Box 103030 Med. Ctr., Duke University, Durham, NC 27710. Tel.: 919-668-7641; Fax: 919-613-5145; E-mail: geoffrey.pitt@duke.edu.

[2] The abbreviations used are: KChIP, potassium channel interacting protein; mEPSC, miniature excitatory postsynaptic current; mIPSC, miniature inhibitory postsynaptic current; APV, 2-amino-5-phosphonovaleric acid; DNQX, 6,7-dinitroquinoxaline-2,3-dione; BLA, basolateral nucleus of the amygdala; sIPSC, spontaneous inhibitory postsynaptic current; sEPSC, spontaneous excitatory postsynaptic current; d.i.v., days *in vitro*.

pal neurons because KChIP2 is concentrated in their apical and basal dendrites, where it co-localizes with Kv4.2 (11), yet the effect of KChIP2 deletion on I_A in hippocampal neurons has not been investigated. We also evaluated the physiological consequences of KChIP2 deletion, considering the hypothesis that an effect on I_A might influence the development of limbic seizures because of the importance of the hippocampus in networks involving limbic seizures.

EXPERIMENTAL PROCEDURES

Animals—The generation of *Kchip2*$^{+/-}$ mice was previously described (12), as was their rederivation (13) in a mixed 129SV and Black Swiss background. Heterozygotes were bred to generate WT or *Kchip2*$^{-/-}$ animals, which were then maintained as separate lines. WT and *Kchip2*$^{-/-}$ mice used for the experiments in this report have the identical genetic background, and any differences in responses between WT and *Kchip2*$^{-/-}$ mice to the kindling induced seizures are background-independent. Adult (male, 7–10 months) and 5–6-week-old (male and female) WT and *Kchip2*$^{-/-}$ mice were used for kindling and brain slice experiments, respectively. Dissociated hippocampal neuron cultures were obtained from newborn (postnatal days 1 and 2) pups. The animals were handled according to National Institutes of Health Guide for the Care and Use of Laboratory Animals. The study was approved by Duke University and Durham Veterans Affairs Medical Center Animal Care and Welfare Committees.

Surgery and Kindling—Procedures for surgery and kindling were performed as described previously (14, 15) by an individual blinded to the genotypes of the animals. Briefly, under pentobarbital (60 mg/kg) anesthesia, a bipolar electrode used for stimulation and recording was stereotactically implanted in the right amygdala. Following a postoperative recovery period of ~1 week, the electrographic seizure threshold in the amygdala was determined, and stimulations at the intensity of the electrographic seizure threshold were subsequently administered twice daily, 5 days per week. Electroencephalographic and behavioral manifestations of seizures were classified according to a modification of the description of Racine (16) as previously described (14, 15): 1, facial clonus; 2, head nodding; 3, unilateral forelimb clonus; 4, rearing with bilateral forelimb clonus; 5, rearing and falling (loss of postural control); 6, running or bouncing seizures; and 7, tonic hind limb extension. The mice were stimulated until fully kindled as defined by the occurrence of three consecutive seizures of class 4 or greater. Unstimulated control animals of each genotype underwent surgical implantation of an electrode in amygdala and were handled identically but were not stimulated. Accuracy of electrode placement was verified by histological analysis, and only animals with correct electrode placement in the amygdala were included in the statistical analysis for kindling experiment.

Hippocampal Neuronal Cultures—Hippocampi from 1–2-day newborn WT and *Kchip2*$^{-/-}$ mice were dissociated through enzymatic treatment with 0.25% trypsin and subsequent trituration. The cells were plated on glass coverslips previously coated with poly-D-lysine and laminin in 12-well cell culture plate in the density of 100,000/ml. Hippocampal cells were grown in neurobasal A medium (Invitrogen) supplemented with 2% B27, 2 mM glutamine, 10% heat-inactivated fetal bovine serum, and 1% penicillin/streptomycin in 5% CO_2 incubator at 37 °C overnight, and then this medium was replaced by one containing 2% B27, 0.5 mM glutamine, 1% heat-inactivated fetal bovine serum, 70 μM uridine, and 25 μM 5-fluorodeoxyuridine.

Electrophysiology of Dissociated Hippocampal Neuronal Culture—Electrophysiological recordings were performed at room temperature. Inhibitory and excitatory synapses form and maturate within 12 days *in vitro* (d.i.v.) in dissociated hippocampal neuronal cultures (17). To conduct multiple experiments (*i.e.*, obtain I_A parameters, quantify spontaneous firing and evoked action potentials, and measure synaptic currents) from cultures plated at same day and thereby eliminate culture selection bias from the different parameters evaluated, we performed experiments sequentially in the following time frames: I_A recordings were performed on cultures at 10–13 d.i.v.; analysis of spontaneous firing and action potential was performed on cultures at 14–18 d.i.v.; and miniature inhibitory postsynaptic currents (mIPSCs) and miniature excitatory postsynaptic currents (mEPSCs) were performed on cultures at 16–19 d.i.v. I_A, mIPSCs, and mEPSCs were obtained from hippocampal pyramidal shape neurons in the whole cell voltage patch clamp configuration with an Axopatch 200B amplifier at a holding potential of −70 mV. Spontaneous firing and action potential were recorded in the whole cell current patch clamp mode. The current clamp recordings were held at 0 current. Currents and potentials were sampled at 10 kHz and filtered at 2 kHz.

For I_A, spontaneous firing, action potential, and mEPSC recordings, the pipette internal solution contained 120 mM potassium gluconate, 10 mM KCl, 5 mM $MgCl_2$, 0.6 mM EGTA, 5 mM HEPES, 0.006 mM $CaCl_2$, 10 mM phosphocreatine disodium, 2 mM Mg-ATP, 0.2 mM GTP, and 50 units/ml creatine phosphokinase, pH 7.2 adjusted with KOH; for mIPSC recordings, the pipette internal solution contained 115 mM KCl, 5 mM $MgCl_2$, 10 mM EGTA, 5 mM HEPES, 2 mM Mg-ATP, 0.2 mM Na-ATP, 5 mM phosphocreatine disodium, pH 7.3, adjusted with KOH. External solution for I_A contained 119 mM NaCl, 3 mM KCl, 20 mM HEPES, 2 mM $CaCl_2$, 1 mM $MgCl_2$, 30 mM glucose, 0.0005 mM tetrodotoxin, 2 mM CsCl, 5 mM tetraethylammonium chloride, 0.1 mM $CdCl_2$, and synaptic blockers, 0.05 mM 2-amino-5-phosphonovaleric acid (APV), 0.02 mM 6,7-dinitroquinoxaline-2,3-dione (DNQX), and 0.1 mM picrotoxin, pH 7.3, adjusted with NaOH. Basic external solution for spontaneous firing, action potential, and mIPSC and mEPSC recordings contained 126 mM NaCl, 3 mM KCl, 20 mM HEPES, 2 mM $CaCl_2$, 1 mM $MgCl_2$, 30 mM glucose, pH 7.3, adjusted with NaOH. For spontaneous firing and action potential, 0.002 mM glycine was added to the basic solution; for mIPSC recording, 0.001 mM tetrodotoxin, 0.05 mM APV, and 0.02 mM DNQX were added; for mEPC recording, 0.001 mM tetrodotoxin, 0.002 mM glycine, and 0.1 mM picrotoxin were added.

To isolate I_A, total outward K^+ currents and the slow activating and slow inactivating components were recorded separately in the same neuron with two different protocols (18). Total outward K^+ currents were induced by steps from −90 to +50 mV in 10-mV increments over 400 ms after a 100-ms step to −130 mV from the holding potential. Slowly activating and

slowly inactivating components were obtained with a 100-ms prepulse to −10 mV before the steps from −90 to +50 mV. I_A was yielded by subtracting the slowly activating and inactivating components from the total K^+ currents. Activation curves were obtained using a Boltzmann function: $G/G_{max} = (1 + \exp(-(V - V_{½})/k))^{-1}$, where G/G_{max} is the conductance normalized to its maximal value, V is the membrane potential, $V_{½}$ is the membrane voltage at which the current amplitude is half-maximal, and k is the slope factor. Steady-state inactivation was tested by a two-pulse protocol with the first pulse of 400 ms from −100 to −10 mV in 10-mV increments followed by a second pulse fixed at +10 mV. I_A induced by the second pulse was normalized to the maximal current and plotted as the function of the voltages initiated by the first pulse, which was fitted with the Boltzmann function: $I/I_{max} = (1 + \exp((V - V_{½})/k))^{-1}$, where I/I_{max} is the normalized value. Another two-pulse protocol was adopted to test A-type channel recovery from inactivation. Both pulses 1 and 2 were depolarized to +10 mV with various intervals ranging from 1 to 600 ms between them. I_A were separated from noninactivating sustained K^+ currents by setting the base line as the current level at the end of P2 at the shortest interval of 1 ms. Currents induced by P2 over that by P1 (I_2/I_1 ratios) were plotted as a function of the various intervals. Recovery τ was estimated with first order exponential decay: $y = y_0 + Ae^{-x/t}$, where y_0 indicates y offset, A indicates amplitude, and t indicates time constant.

Series resistance for voltage patch clamp experiments ranged from 6 to 15 MΩ (WT, 10.0 ± 1.0 MΩ; *Kchip2*$^{-/-}$, 10.6 ± 0.9 MΩ) with 40–60% correction. Junction potential in current patch clamp experiments was measured immediately after recording by quickly detaching pipette from the recorded cell. The measured junction potential was 2.0 ± 0.5 mV for WT neurons and 2.1 ± 0.9 mV for *Kchip2*$^{-/-}$ neurons, which was not corrected.

Electrophysiology of Brain Slice—The animals were deeply anesthetized with isoflurance. The brain was quickly removed from the skull after decapitation and immediately chilled in an ice-cold, oxygenated artificial cerebrospinal fluid containing 120 mM NaCl, 3.3 mM KCl, 25 mM $NaHCO_3$, 1.23 mM NaH_2PO_4, 1.8 mM $CaCl_2$, 1.2 mM $MgSO_4$, and 10 mM glucose. Coronal slices (300-μm thickness) containing the hippocampus or the basolateral nucleus of the amygdala (BLA) were cut with a moving blade microtome and were kept in normal oxygenated artificial cerebrospinal fluid at 35 °C for 60 min. The slices were then kept at room temperature until used for recording.

A single slice was transferred to the recording chamber constantly perfused (~3 ml/min) with oxygenated artificial cerebrospinal fluid at 35 °C. The neurons were viewed under a Zeiss upright microscope equipped with a 40× water immersion objective and an enhanced differential interference contrast video microscope system. Recording electrodes with resistance of 4–8 MΩ were pulled from borosilicate glass capillaries (1.5 mm outer diameter) using a P87 electrode puller. Access resistance and input capacitance were electronically compensated by ~60–70% and monitored throughout the experiment to confirm the stability of the recording. The signals were filtered at 5 kHz and digitized at 10 kHz through a Digidata1440 interface controlled by pClamp10 software (Molecular Devices).

Spontaneous and evoked action potentials in CA1 and BLA pyramidal neurons were recorded under whole cell current clamp configuration. Evoked action potentials were induced by injecting a series of depolarization current with 600-ms duration in 10-pA increments from a holding potential of −70 mV. The minimal current injected that could evoke action potentials was defined as the current threshold for individual neurons from WT or *Kchip2*$^{-/-}$ mice. Spontaneous inhibitory and excitatory postsynaptic currents (sIPSCs and sEPSCs) were recorded from soma in hippocampal CA1 pyramidal neurons under whole cell voltage clamp mode at a holding potential of −70 mV. sIPSCs were isolated in the presence of APV (50 μM) and DNQX (20 μM), and sEPSCs were obtained in the presence of APV (50 μM) and picrotoxin (75 μM). All internal pipette solutions for slice recording were same as those used in the experiments with cultured hippocampal neurons.

Quantitative PCR Analysis—Total mRNA was purified from hippocampal tissue from 5-month-old mice using the RNAeasy Plus mini kit (Qiagen). The primers are: for Kchip1, forward 5′-TCAAAAACGAGTGCCCTAGC, reverse 5′-CAGAGCAGTCACAAAGTCCTCG; for Kchip2, forward 5′-ATGGCTGTATCACGAAGGAGG, reverse 5′-CCGTCCTTGTTTCTGTCCATC; for Kchip3, forward 5′-GGAGATCCTGGGCGCATAC, reverse 5′-GTGAACCGTGGCCTTTGC; for Kchip4, forward 5′-AGCAGTTCTGATCGTCATTGTGC, reverse 5′-GCTGTCTTCTAAACCTGCTTCAATC; and for β-actin, forward 5′-GATCAAGATCATTGCTCCTCCTG, reverse 5′-AGGGTGTAAAACGCAGCTCA. Real time PCR quantification was performed using the Applied Biosystems 7300 Real-Time PCR System (Invitrogen). The relative amount of target message in each reaction was determined from the detection threshold cycle number (C_t), which is inversely correlated with the abundance of the initial level of the message, after normalization to the C_t for actin, obtained in the same experiment.

Statistics—The numerical averages are presented as the means ± S.E. The cumulative amplitude distributions of synaptic currents were analyzed with Kolmogorov-Smirnov comparisons, and statistical significance for other parameters was calculated using the unpaired two-sample Student's t test.

RESULTS

Enhanced Seizure Susceptibility—Because loss of I_A via deletion of *Kv4.2* increased susceptibility to seizures in response to convulsant stimuli (19), we hypothesized that deletion of KChIP2 protein might similarly enhance susceptibility to seizures evoked by brief, low intensity trains of electrical stimulation applied to the right amygdala in the kindling model, if KChIP2 were a significant regulator of I_A. There were no observable behavioral alterations in *KChIP2*$^{-/-}$ mice, and there were no spontaneous seizures observed while handling WT or *Kchip2*$^{-/-}$ mice before kindling. In electroencephalographic recordings, no significant differences were detected in the current required to evoke an initial electrographic seizure (210 ± 25 μA *versus* 168 ± 28 μA, respectively; $p = 0.31$) between WT and *Kchip2*$^{-/-}$ mice ($n = 5$ and 9, respectively). Likewise no significant differences were detected in the dura-

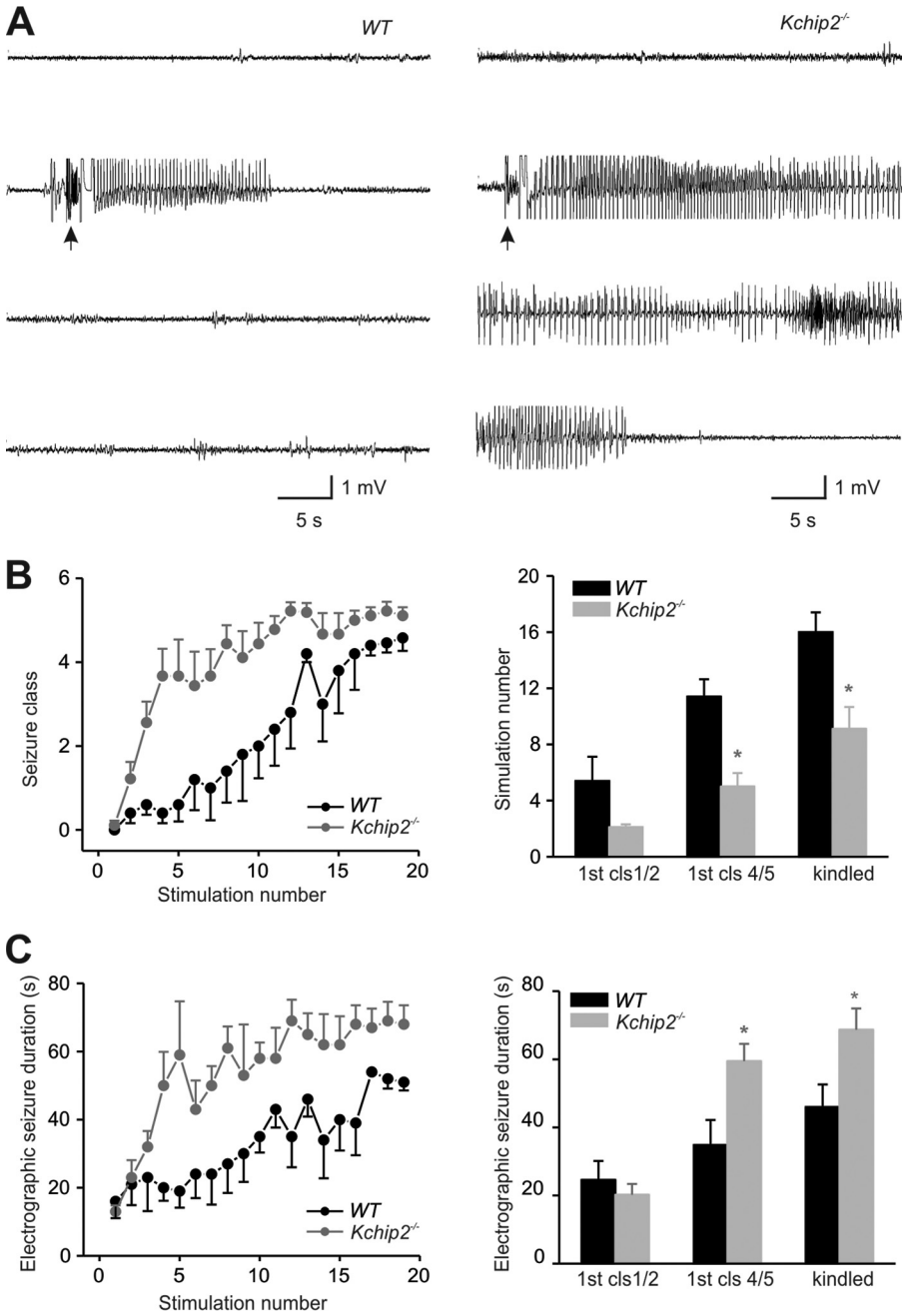

FIGURE 1. **Acceleration of kindling development in *Kchip2*$^{-/-}$ mice.** *A*, electroencephalograms showing the examples of electrographic seizure induced by the fifth stimulation from WT and *Kchip2*$^{-/-}$ mice. The *arrow* represents stimulation. A class 2 seizure (in WT mouse) and a class 4 seizure (in *Kchip2*$^{-/-}$ mouse) accompanied these electrographic seizures. *B*, behavioral seizure class of kindling development. The *right panel* shows number of stimulations required to induce the first time seizure for different seizure classes. Fully kindled stage was defined by the occurrence of three consecutive seizures of class 4 or greater. *C*, electrographic seizure duration. The *right panel* shows the electrographic seizure duration for the first seizure induced at the indicated seizure classes. The stimulation number in the *left panels* of both *B* and *C* refers to the number of stimulations that evoked an electrographic seizure with duration of at least 5 s. *cls*, class.

tion of the initial evoked electrographic seizure (16.0 ± 4.5 *versus* 12.6 ± 1.8 s; $p = 0.54$) between WT and *Kchip2*$^{-/-}$ mice. However, striking increases in behavioral and electrographic seizure responses to subsequent stimulations were evident in *Kchip2*$^{-/-}$ compared with WT mice (Fig. 1). The number of stimulations required to evoke the initial class 4 or 5 seizure was decreased by >2-fold in *Kchip2*$^{-/-}$ mice (5.0 ± 1.0) compared with WT controls (11.4 ± 1.2; $p = 0.005$). Likewise the number of stimulations required to induce the third consecutive clonic tonic seizure (class 4 or greater) was significantly decreased (9.1 ± 1.6 for *Kchip2*$^{-/-}$ and 16.0 ± 1.4 for WT mice, respectively; $p = 0.01$) (Fig. 1*B*). The duration of electrographic seizures accompanying the behavioral seizures in *Kchip2*$^{-/-}$ mice exceeded that of WT controls (Fig. 1, *A* and *C*), evident in the average duration accompanying the first class 4 or 5 seizure of 59.4 s in *Kchip2*$^{-/-}$ mice compared with 34.8 s in WT mice ($p = 0.04$). Thus, despite similar excitability in the naïve condition as assessed by electrographic seizure threshold and duration of

the initial electrographic seizure, the absence of KChIP2 enhanced epileptogenesis as revealed by a more rapid rate of development of kindling. These stark differences strongly implicate KChIP2 as nonredundant in at least some sets of neurons.

Diminished I_A in Hippocampal Neurons—Although a previous study has suggested a lack of effect of KChIP2 deletion on I_A in posterior cortical neurons, we asked whether I_A in hippocampal neurons might be sensitive to the absence of KChIP2. Among the KChIP proteins, KChIP2 is especially highly expressed within the apical and basal dendrites of hippocampal pyramidal cells (11). We therefore recorded I_A in cultured hippocampal neurons from *Kchip2*$^{-/-}$ and WT animals using a two-step procedure (18). After recording total K^+ current, we isolated the residual slowly activating component in the same neuron by eliminating the fast activating I_A component with a prepulse to a −10 mV. We then subtracted the slowly activating component from the total K^+ current to yield I_A. As shown in the *inset* of Fig. 2*A*, we confirmed the identity of this current as I_A by showing that it was completely blocked by 4-aminopyridine in WT and *KChIP2*$^{-/-}$ neurons. With this method, Fig. 2 (*A* and *B*) shows that KChIP2 deletion reduced I_A amplitude with the strongest depolarizations (>40 mV; $p = 0.04$), but the overall effect was mild. Previous studies have demonstrated that KChIP proteins increase Kv4 channel availability (depolarizing shift in steady-state inactivation) and enhance channel recovery from inactivation while having a minimal effect upon channel activation (1, 20). We therefore assessed whether any of these I_A gating kinetics were altered by elimination of KChIP2. Consistent with those previous observations, deletion of KChIP2 did not affect channel activation (Fig. 2*C*) but did shift the $V_{½}$ for steady-state inactivation (−54.7 ± 1.1 *versus* −59.7 ± 1.1 mV; $p = 0.004$) (Fig. 3, *A* and *B*) and slowed recovery from inactivation (τ = 23.2 ± 2.5 *versus* 32.3 ± 2.2 ms, respectively; $p = 0.01$) (Fig. 3, *C* and *D*). Although these data suggest that the absence of KChIP2 imparts only a mild decrease to I_A amplitude, they demonstrate significant effects upon I_A availability and recovery from inactivation in hippocampal neurons. To test whether other Kv currents were affected, we analyzed the residual slowly activating component. No significant difference was found between WT and *Kchip2*$^{-/-}$ neurons (data not shown). Together, these observations show that KChIP2 is an important regulator of I_A in hippocampal neurons and provide additional evidence that there is no redundancy for KChIP2 in hippocampal pyramidal neurons.

Increased Excitability in Hippocampal Neurons in Dissociated Hippocampal Culture and Brain Slice Preparation—What are the physiological consequences of these effects upon I_A? We first tested in dissociated hippocampal culture whether absence of KChIP2 affected spontaneous firing, an important parameter for neuronal excitability. WT neurons were relatively quiet, firing only occasional single action potentials. In contrast, the average spontaneous firing rate (spikes/s) was almost 10-fold greater in *Kchip2*$^{-/-}$ neurons (2.8 ± 0.5 s^{-1} for *Kchip2*$^{-/-}$ *versus* 0.3 ± 0.1 s^{-1} for WT neurons; $p = 0.0001$). This spontaneous activity consisted of single as well as complex action potentials (Fig. 4, *A* and *B*). The increase in spontaneous activity did not result from a change in resting membrane potential,

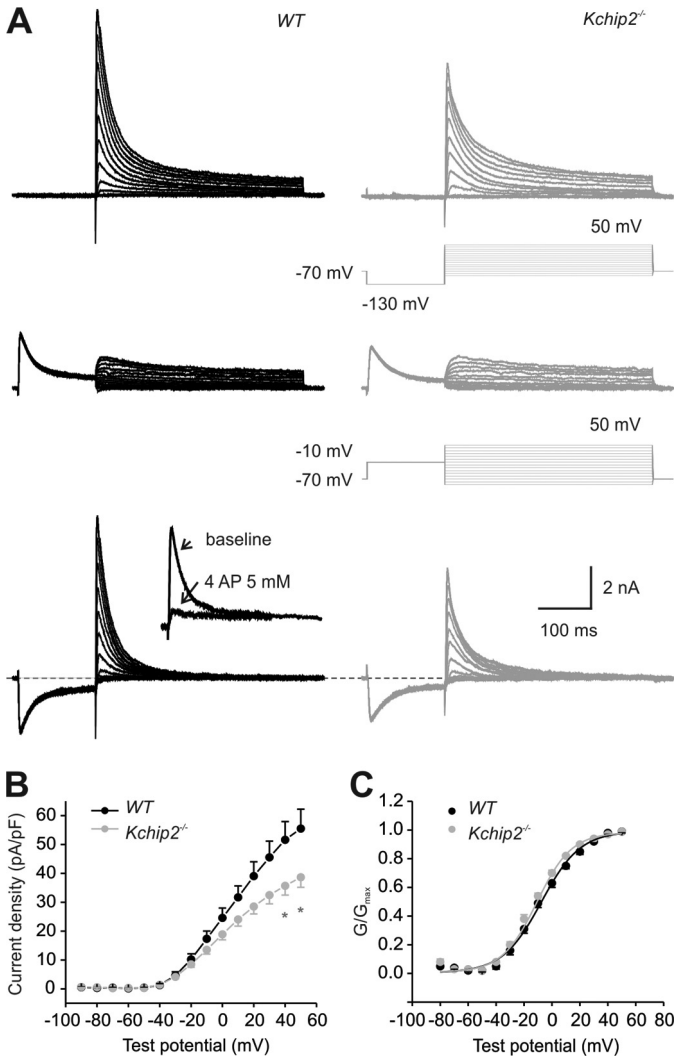

FIGURE 2. **Voltage-dependent activation of I_A in cultured hippocampal pyramidal neurons.** *A*, example current traces and protocols for isolating I_A from WT and *Kchip2*$^{-/-}$ neurons. The *upper row* shows total outward K^+ currents evoked by 400-ms depolarization steps from −90 to +50 mV in 10-mV increments following a −130-mV hyperpolarization step of 100-ms duration from a holding potential of −70 mV; the *middle row* shows that the currents were induced by the 400-ms depolarization steps from −90 to +50 mV in 10-mV increments following a predepolarization pulse to −10 mV, by which the fast activating and fast inactivating component was eliminated. The slow inactivated and noninactivated components of the total outward K^+ currents remained. The *bottom row* shows the fast activating and fast inactivating I_A derived from subtraction of the currents in *middle row* from the total outward K^+ currents in the *upper row*. *Inset*, I_A was blocked by 5 mM 4 AP, A-type channel blocker. *B*, summarized peak current amplitudes ($n = 14$ for WT, $n = 19$ for *Kchip2*$^{-/-}$; *, $p < 0.04$). *C*, voltage-dependent activation curve.

which was similar between the two groups (−71.7 ± 1.2 mV for WT *versus* −70.2 ± 1.7 mV for *Kchip2*$^{-/-}$), nor from a difference in input resistance (123 ± 10.9 *versus* 161.2 ± 22.4 MΩ; $p = 0.14$). Moreover, injection of depolarizing current for 5 ms elicited single action potentials in WT and *Kchip2*$^{-/-}$ neurons (Fig. 4*C*) that were indistinguishable in standard action potential parameters (Table 1). The input resistance and half-width of induced action potentials trended higher in *KChIP2*$^{-/-}$ neurons, but the changes were not statistically significant. This suggested that the increased spontaneous activity in *Kchip2*$^{-/-}$ neurons in cultured hippocampal neurons was mostly synaptically driven. Indeed, application of DNQX, an 2-amino-3-(3-

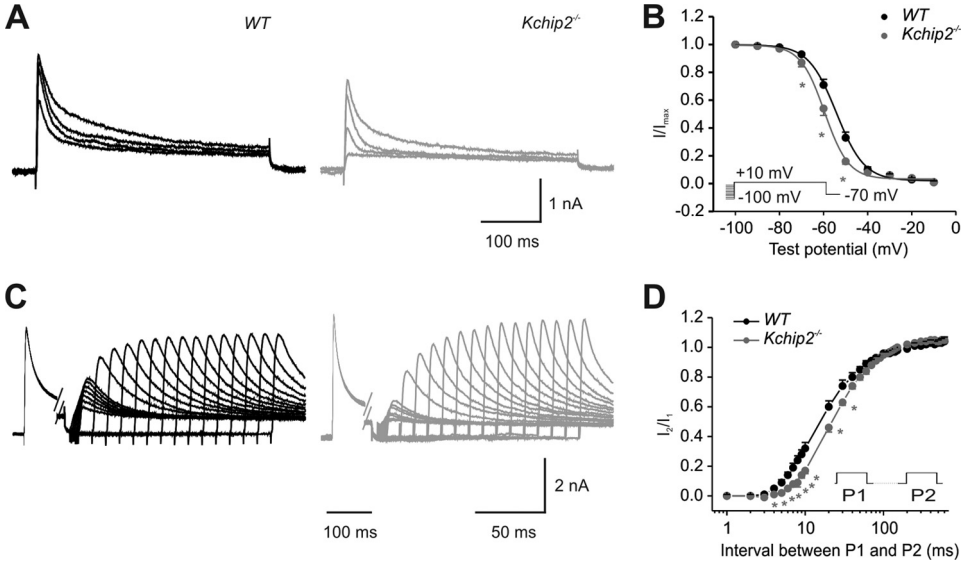

FIGURE 3. **Steady-state inactivation and recovery from inactivation of I_A in cultured hippocampal pyramidal neurons.** *A* and *B*, steady-state inactivation of I_A, measured by a two-pulse stimulation with a 400-ms first pulse from −100 to −10 mV followed by a second pulse at +10 mV. I_A induced by the second pulse were normalized to the maximum current and plotted as the function of the voltages initiated by the first pulse. Examples of I_A induced by the second pulse following a first pulse at V_{test} of −100, −70, −60, or −50 mV recorded in WT and *Kchip2*$^{-/-}$ neurons are shown in *A*. I_A steady-state inactivation fitted with Boltzmann equation is shown in *B* ($n = 13$ for WT, $n = 15$ for *Kchip2*$^{-/-}$; *, $p = 0.004$). *C*, examples of recovery from inactivation in WT and KChIP2 deleted neurons. The recovery from inactivation was tested by a two-pulse stimulation protocol to +10 mV with the intervals ranging from 1 to 600 ms between the two pulses. *D*, I_2 over I_1 ratio at various intervals ($n = 14$ for WT, $n = 12$ for *Kchip2*$^{-/-}$; *, $p \leq 0.02$). *P1*, pulse 1; *P2*, pulse 2.

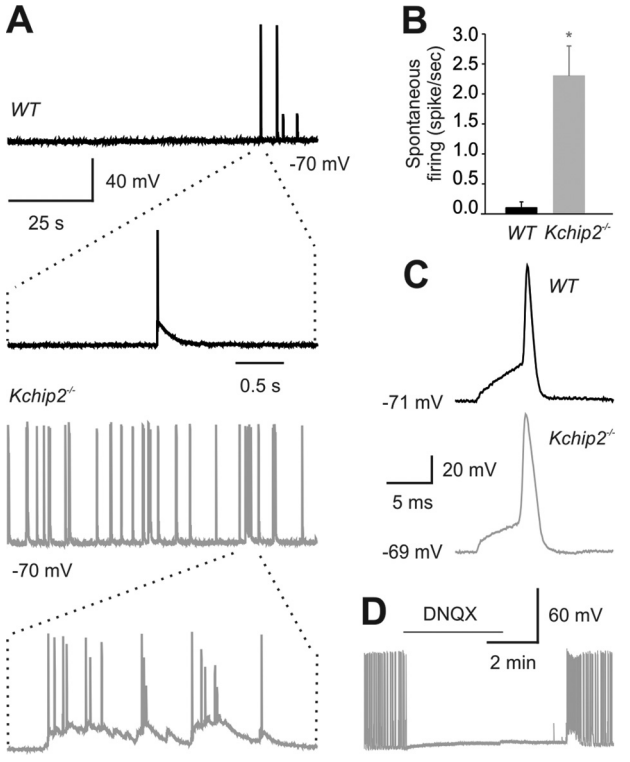

FIGURE 4. **Spontaneous and evoked action potentials in cultured hippocampal neurons.** *A*, examples of spontaneous action potentials from WT and *Kchip2*$^{-/-}$ neurons. *B*, summarized spontaneous firing rate ($n = 20$ for both; *, $p = 0.0001$). *C*, examples of action potentials evoked by a 5-ms depolarization step in WT and *Kchip2*$^{-/-}$ neurons. *D*, spontaneous firing in KChIP2 deleted neuron was completed blocked by 20 μM 2-amino-3-(3-hydroxy-5-methyl-isoxazol-4-yl)propanoic acid receptor blocker DNQX.

hydroxy-5-methyl-isoxazol-4-yl)propanoic acid receptor antagonist, completely silenced the spontaneous activity in *Kchip2*$^{-/-}$ neurons (Fig. 4*D*). These data suggest that KChIP2 is crucial for the maintenance of homeostatic excitability in hippocampal pyramidal neurons.

TABLE 1

Action potential induced by 5-ms depolarization

AMP, peak amplitude; TH, threshold, the voltage at which action potential was evoked, HD, half duration, the width of action potential at the level of 50% AMP; RT, rise time, from 10 to 99% of rising phase; DT, decay time, from 99 to 10% of repolarization phase.

	AMP	TH	HD	RT	DT	*N*
	mV	*mV*	*ms*	*ms*	*ms*	
WT	105 ± 1.4	−41 ± 1.6	1.3 ± 0.1	4.7 ± 0.2	1.8 ± 0.1	21
KChip2$^{-/-}$	100 ± 2.7	−40 ± 1.5	1.6 ± 0.1	4.9 ± 0.1	2.2 ± 0.3	22

We next investigated whether the increased excitability in *Kchip2*$^{-/-}$ hippocampal pyramidal neurons was present in slice preparations. Although we observed spontaneous firing in all 12 CA1 pyramidal neurons from *Kchip2*$^{-/-}$ mice, we observed no spontaneous firing in pyramidal neurons from WT mice (Fig. 5, *A* and *B*). Further, the threshold to evoke an action potential in *Kchip2*$^{-/-}$ neurons (−63 ± 1.3 mV) was significantly lower than in WT neurons (−54 ± 1.2 mV; $p = 0.0002$ compared with *Kchip2*$^{-/-}$) as shown in Fig. 5*C*. This increased excitability in *Kchip2*$^{-/-}$ neurons appeared to be region-specific, because we observed no spontaneous action potentials in BLA neurons from WT or *Kchip2*$^{-/-}$ neurons (Fig. 5, *A* and *B*). Moreover, the threshold potential was not different between WT and *Kchip2*$^{-/-}$ in BLA neurons (51 ± 0.4 mV for WT *versus* 52 ± 0.8 mV for *Kchip2*$^{-/-}$; $p = 0.23$), as shown in Fig. 5*C*.

We further confirmed the increased excitability in *Kchip2*$^{-/-}$ hippocampal neurons by measuring the minimal stimulation intensity necessary to induce action potentials (during a series of 600-ms depolarization steps). CA1 pyramidal neurons from *Kchip2*$^{-/-}$ mice required a lower stimulation intensity (39 ± 7.8 pA) than WT (76 ± 15.3 pA; $p = 0.04$) (Fig. 5, *D* and *E*). Consistent with the regional specific differences

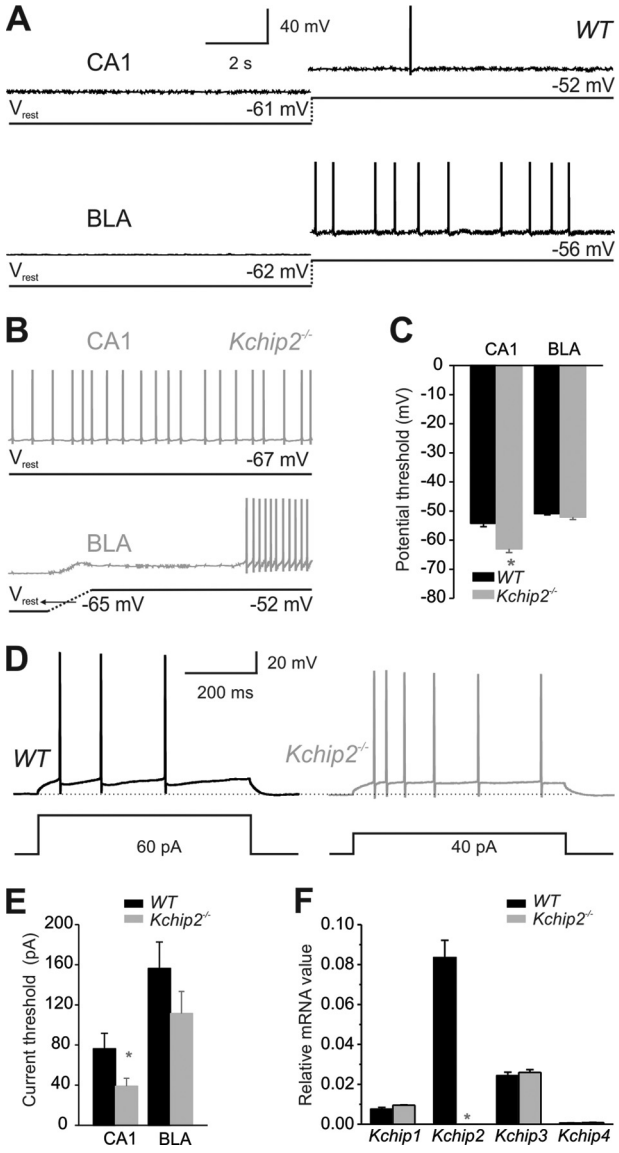

FIGURE 5. **Spontaneous and evoked action potentials in CA1 and BLA pyramidal neurons in brain slices.** *A*, current clamp recording in CA1 and BLA pyramidal neurons from WT mice. *B*, current clamp recording in CA1 and BLA pyramidal neurons from *Kchip2*$^{-/-}$ mice. Spontaneous action potentials were only observed in CA1 pyramidal neurons from *Kchip2*$^{-/-}$ mice. Current injection was required to induce action potentials in WT CA1 and WT and *Kchip2*$^{-/-}$ BLA pyramidal neurons. *C*, average threshold potential for CA1 (WT, $n = 7$; *Kchip2*$^{-/-}$, $n = 12$; *, $p = 0.0002$) and BLA (WT, $n = 5$; *Kchip2*$^{-/-}$, $n = 6$; $p = 0.23$) pyramidal neurons. *D*, examples of action potentials (at the current threshold) evoked in CA1 pyramidal neurons for WT and *Kchip2*$^{-/-}$. *E*, average threshold currents required for action potentials induced by a 600-ms depolarization in CA1 (WT, $n = 8$; *Kchip2*$^{-/-}$, $n = 10$; *, $p = 0.04$) and BLA (WT, $n = 8$; *Kchip2*$^{-/-}$, $n = 7$; $p = 0.22$) pyramidal neurons. *F*, mRNA levels of *Kchip1*, *Kchip2*, *Kchip3*, and *Kchip4* measured with quantitative PCR in hippocampi from WT and *Kchip2*$^{-/-}$ mice ($n = 5$).

observed for spontaneous action potentials and the action potential threshold, there was no significant difference in the stimulation intensity in BLA between WT and *Kchip2*$^{-/-}$ neurons (156 ± 26.1 pA *versus* 111 ± 22.0 pA, respectively; $p = 0.22$) (Fig. 5, *D* and *E*). Thus, these results from brain slices extend and confirm those obtained from cultured neurons, showing that hippocampal pyramidal neurons are more excitable in *Kchip2*$^{-/-}$ mice and suggesting that KChIP2 regulation of I_A is region-specific.

The marked differences in regional excitability suggested insufficient compensatory regulation by other KChIP isoforms, if any, in *Kchip2*$^{-/-}$ hippocampus. This would stand in contrast to results reported in posterior cortical neurons (10) and suggested regional specific regulation of KChIP transcription levels. We measured the mRNA levels of *Kchip1*, *Kchip2*, *Kchip3*, and *Kchip4* in hippocampi isolated from adult mice by reverse transcriptase quantitative PCR. As expected based on previous studies of the patterns of KChIP expression (11), we found that *Kchip2* was the most highly expressed KChIP in hippocampus and that there was no detectable *Kchip2* mRNA in *Kchip2*$^{-/-}$ hippocampi (Fig. 5*F*). For the other KChIPs, we did not observe any differences between WT and *Kchip2*$^{-/-}$ hippocampi (Fig. 5*F*). Thus, unlike in posterior cortical neurons (10), other KChIPs do not compensate for the absence of *KChip2* in hippocampus, providing a basis for the regional increased excitability.

Homeostatic Changes—Recent studies have shown that neurons can detect changes in their own firing rates through a set of calcium-dependent sensors that then regulate receptor trafficking to increase or decrease the accumulation of synaptic receptors at synaptic sites (21). The resultant altered activity leads to network-wide changes in activity that generate network-wide adjustments in the balance between excitation and inhibition (22). Therefore, we first measured miniature synaptic currents in cultured hippocampal neurons. We found a significant increase in mIPSC amplitudes ($p = 0.006$) and a shift in the cumulative amplitude distribution in *Kchip2*$^{-/-}$ neurons ($p < 0.001$). These results are similar to what was observed when the I_A pore-forming *Kv4.2* subunit was deleted (23). There was no change in mEPSC amplitude (Fig. 6). The mIPSC frequency was also increased ($p = 0.006$), whereas the mEPSC frequency was reduced in *Kchip2*$^{-/-}$ neurons ($p = 0.02$), suggesting additional presynaptic mechanisms. Thus, as with deletion of Kv4.2, a chronic decrease in I_A by KChIP2 deletion produced a compensatory up-regulation of inhibitory synaptic activity and a reduced excitatory input.

We evaluated whether these homeostatic changes were also present within the context of hippocampal brain slices, in which network architecture and intrinsic synaptic connections are preserved by recording sIPSCs and sEPSCs in CA1 pyramidal neurons. We found that in *Kchip2*$^{-/-}$ mice, the frequency (8 ± 0.8 Hz *versus* 3 ± 0.6 Hz; $p = 0.0003$), amplitude (100 ± 12.8 pA *versus* 65 ± 4.6 pA; $p = 0.04$), and amplitude distribution ($p < 0.001$) of sIPSCs increased in pyramidal neurons from *Kchip2*$^{-/-}$ mice (Fig. 7), consistent with what we observed in cultured hippocampal neurons (Fig. 6). In contrast, there was no significant difference between WT and *KChIP2*$^{-/-}$ mice in either sEPSC frequency (6 ± 1.1 Hz *versus* 4 ± 1.1 Hz; $p = 0.33$) or amplitude (26 ± 2.3 pA *versus* 30 ± 5.0 pA; $p = 0.75$) (Fig. 7). These data further demonstrate that chronic higher activity in pyramidal neurons leads to up-regulation of inhibitory synaptic activity in the hippocampi of *KChIP2*$^{-/-}$ mice.

DISCUSSION

The essential role of I_A in synaptic physiology was firmly established through pharmacological blockade (24) and gene

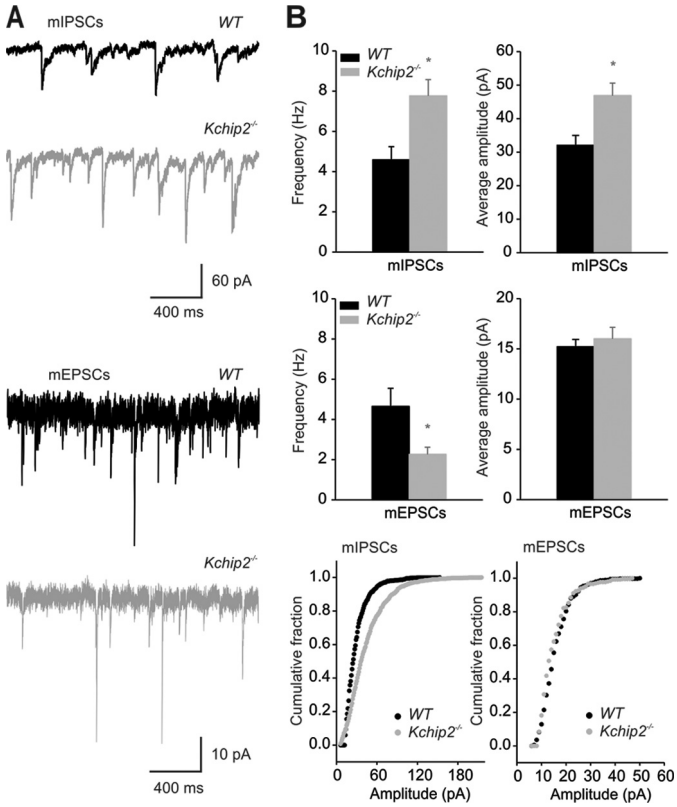

FIGURE 6. **mIPSCs and mEPSCs in cultured hippocampal neurons.** *A*, examples of mIPSC and mEPSCs. *B*, summarized frequency and average amplitude of mIPSC (WT, $n = 11$; *Kchip2*$^{-/-}$, $n = 11$; *, $p = 0.006$ for both frequency and amplitude) and mEPSC (WT, $n = 20$; *Kchip2*$^{-/-}$, $n = 21$; *, $p = 0.02$ for frequency and 0.58 for amplitude) and cumulative distributions of amplitude for mIPSCs ($p < 0.001$) and mEPSCs ($p = 1.0$).

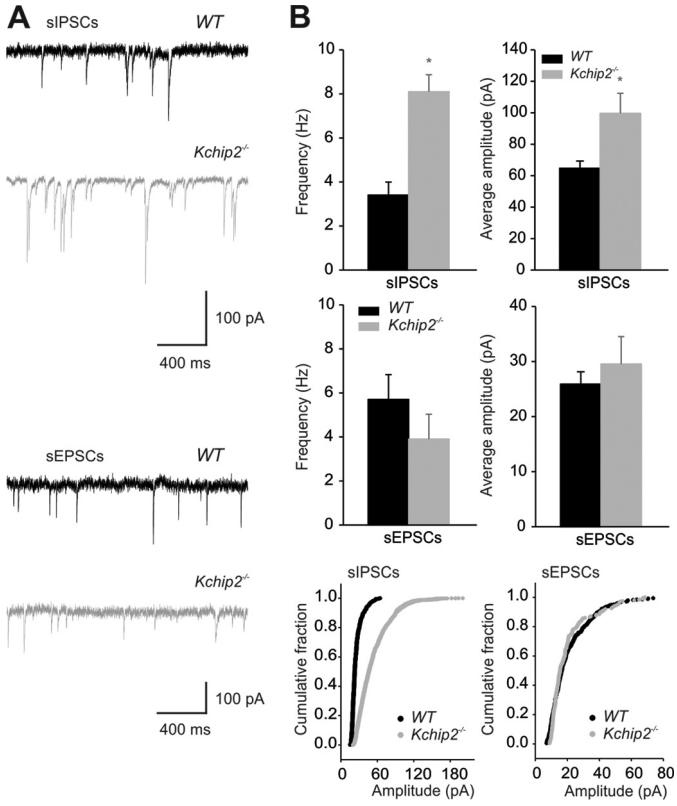

FIGURE 7. **sIPSCs and sEPSCs in CA1 pyramidal neurons in brain slices.** *A*, examples of sIPSCs and sEPSCs. *B*, summarized frequency and average amplitude of sIPSC (WT, $n = 8$; *Kchip2*$^{-/-}$, $n = 12$; *, $p = 0.0003$ for frequency and 0.04 for amplitude) and sEPSC (WT, $n = 11$; *Kchip2*$^{-/-}$, $n = 6$; $p = 0.33$ for frequency and 0.75 for amplitude) and cumulative distributions of amplitude for sIPSCs ($p < 0.001$) and sEPSCs ($p = 0.18$).

deletion of the pore-forming Kv4.2 channel subunit (25). Moreover, the role of I_A in regulating neuronal excitability has been underscored by the demonstration that development of temporal lobe epilepsy is associated with decreased I_A through transcriptional down-regulation of Kv4.2 and increased Kv4.2 phosphorylation by ERK (7) and that *Kv4.2*$^{-/-}$ mice show an increased susceptibility to seizures after injection of kainate (19). Although these studies highlighted the essential nature of Kv4.2, the specific contributions of its auxiliary KChIP subunits were less clear. Knock-out of KChIP2 or KChIP3 is associated with compensatory up-regulation of other KChIP members in posterior cortical neurons, suggesting a functional redundancy among at least some KChIPs in specific neuronal populations (10). The high level of KChIP2 expression in the hippocampus, particularly within the apical dendrites of pyramidal cells, suggested to us that KChIP2 may have a more prominent role in hippocampal I_A, for which the specific contribution of KChIP2 has not been previously investigated. Indeed, we found that KChIP2 deletion affected I_A in hippocampus, as indicated by several independent parameters. These include a reduction in current density, decreased channel availability, and slowed recovery from inactivation. The reduction in current density in *KChIP2*$^{-/-}$ neurons and the slowed recovery from inactivation are consistent with roles established for KChIPs in heterologous expression systems (1), suggesting that another KChIP does not fully replace the loss of KChIP2. The modest diminution in I_A after deletion of the auxiliary KChIP2 subunit, compared with the much larger reduction in I_A with acute pharmacologic blockade or deletion of Kv4.2, is consistent with maintenance of the pore-forming Kv4.2 in these *KChip2*$^{-/-}$ mice.

Nevertheless, these resulting effects upon I_A have important physiological consequences, as shown by the marked (~10-fold) increased spontaneous activity in *Kchip2*$^{-/-}$ hippocampal neurons compared with neurons isolated from wild type mice. Interestingly, this increased spontaneous activity in *KChIP2*$^{-/-}$ mice was not associated with a difference in resting membrane potential or input resistance. Likewise, the kinetics of evoked action potentials were unaffected (although the half-width time tended to increase), as shown in Table 1. These data suggest that the observed increased neuronal excitability was caused by reduced I_A rather than the changes in membrane properties. We hypothesize that the reduced I_A attenuated modulatory effects on synaptic inputs and amplitude of back-propagated action potentials, as previously suggested for I_A in the context of pharmacological blockade (3, 4), thereby shifting the input-output relationship and contributing to an increase in spontaneous firing. These physiological consequences in the absence of KChIP2 demonstrate that other KChIPs cannot substitute, thereby demonstrating a lack of redundancy among KChIPs in hippocampal neurons. Indeed, quantitative PCR analysis showed no change in the mRNA levels of *Kchip1*,

Kchip3, or *Kchip4* in hippocampi in *Kchip2*$^{-/-}$ mice compared with WT. The increased excitability in cultured hippocampal neurons was confirmed in brain slices. This preparation also demonstrated that the changes are regionally specific and correlate with KChIP2 expression: we did not observe any change in BLA, an area in which KChIP2 expression is not well documented.

Along with the increase in spontaneous firing, we observed an increase in mIPSC frequency and a decrease in mEPSC frequency in cultured *KChip2*$^{-/-}$ neurons. This suggests that deletion of *Kchip2* leads to neuronal programs aimed at stabilizing activity. We also observed a compensatory up-regulation of GABA currents as indicated by increased amplitude of mIPSCs, similar to what was found in the Kv4.2 knock-out model (23). This up-regulation of inhibitory synaptic activity was confirmed in brain slice in which *in vivo* synaptic connections are preserved. Generally, stabilization of neuronal activity includes, for example, activity-dependent regulation of intrinsic neuronal firing; synaptic scaling (which is involved in excitatory pre- and postsynaptic plasticity), the balancing of excitation and inhibition with neuronal networks, and compensatory changes in synaptic receptor and synapse numbers (22). A hallmark of I_A deletion (*i.e.*, in *Kv4.2*$^{-/-}$ mice) is a compensatory up-regulation of inhibitory currents. The consequences of this homeostatic change in *Kv4.2*$^{-/-}$ mice is a relatively small net increase in excitability when compared with the marked increased excitability observed if I_A was acutely blocked by 4-aminopyridine (23, 24). Our observations fit well with these general principles and suggest that the KChIP2 and I_A are parts of a powerful homeostatic synaptic signaling pathway and that KChIP2, an important regulator of I_A in hippocampal pyramidal neurons, plays a crucial role in the maintenance of neuronal homeostatic excitability. Although the mechanisms underlying homeostatic regulation of inhibition have been extensively studied in many systems (26–32), the specific sensors and the downstream signaling cascades in *KChIP2*$^{-/-}$ neurons are not known.

The increased susceptibility of *Kchip2*$^{-/-}$ mice to kindling even though the electrographic seizure thresholds and durations of the initial electrographic seizure were not different between *Kchip2*$^{-/-}$ and WT mice is an additional indication that KChIP2 may be nonredundant in at least some neuronal populations but dispensable in others. The lack of an effect on initial seizure threshold might reflect that deletion of KChIP2 has limited effects on I_A in amygdala (where the seizures initiated). Our data showing a region-specific effect of KChIP2 deletion on intrinsic excitability (and, specifically, no effect in the BLA where kindling is initiated) are entirely consistent with this hypothesis. In contrast, the differences manifested after subsequent stimulations suggest that absence of KChIP2 may affect the limbic-hippocampal circuit, possibly because of the specific effects we observed in isolated hippocampal neurons and CA1 pyramidal neurons in brain slices. In addition, the increased excitability caused by KChIP2 deletion may have triggered both intra- and extrahippocampal compensatory mechanisms to maintain homeostatic excitability, thereby preventing spontaneous seizures or changes to the seizure threshold in *Kchip2*$^{-/-}$ mice. Moreover, the effects of KChIP2 may not be limited to regulation of I_A, as suggested by roles of other KChIPs. KChIP3-deficient mice show both reduced responses in models of acute pain through a transcriptional mechanism and decreased amyloid β production via down-regulatory γ-secretase activity (33, 34), but these effects are not likely through I_A, because KChIP3 also interacts with Alzheimer disease-associated presenilin-2 (2, 35), binds to a downstream regulatory element, and functions as a transcriptional repressor (35, 36).

Although a number of epilepsy syndromes have been associated with loss of function or mutations in ion channel pore-forming subunits (37), the demonstration here that loss of function of a channel modulatory subunit can lead to epilepsy fits within a smaller but growing category. For example, a previous study identified epilepsy-associated mutations or deletion in the Na^+ channel β1b subunit (38, 39). Recently it was reported that the Scn1b-encoded Na^+ channel β1 subunit can interact with Kv4.2 and increase I_A by stabilizing the expression of Kv4.2 in a heterologous system and can regulate neuronal excitability through modulation of Kv4.2 in Scn1b-null cortical pyramidal neurons (40), suggesting that, in addition to the change in sodium currents, reduced I_A may also contribute to the seizures in Scn1b-null mice. Further, mutations of Ca^{2+} channel β4 (41) and the Ca^{2+} channel $\alpha_2\delta$-2 subunit (42) have also been associated with epilepsy. The potential importance of channel modulatory subunits to epilepsy is underscored by the mechanism of action of the gabapentinoids gabapentin and pregabalin, which exert their anticonvulsant action through Ca^{2+} channel $\alpha_2\delta$ subunits (43). Identification of additional modulators, such as KChIP2, offers potential new targets for therapeutic intervention and drug design.

Finally, our demonstration of *KChIP2* as a seizure susceptibility gene may have implications for sudden unexpected death in epilepsy. This entity, which describes the marked increase risk of epilepsy patients (compared with the general population) to die suddenly, has garnered increased attention in the last few years (44). Because *Kchip2*$^{-/-}$ mice were previously shown to be highly susceptible to induced arrhythmias (12), our data suggest that loss of function mutations in an ion channel modulatory subunit could confer an increased susceptibility to both seizures and cardiac arrhythmias, thereby providing a unified mechanism for a neurocardiac syndrome such as sudden unexpected death in epilepsy.

REFERENCES

1. An, W. F., Bowlby, M. R., Betty, M., Cao, J., Ling, H. P., Mendoza, G., Hinson, J. W., Mattsson, K. I., Strassle, B. W., Trimmer, J. S., and Rhodes, K. J. (2000) Modulation of A-type potassium channels by a family of calcium sensors. *Nature* **403,** 553–556
2. Morohashi, Y., Hatano, N., Ohya, S., Takikawa, R., Watabiki, T., Takasugi, N., Imaizumi, Y., Tomita, T., and Iwatsubo, T. (2002) Molecular cloning and characterization of CALP/KChIP4, a novel EF-hand protein interacting with presenilin 2 and voltage-gated potassium channel subunit Kv4. *J. Biol. Chem.* **277,** 14965–14975
3. Hoffman, D. A., Magee, J. C., Colbert, C. M., and Johnston, D. (1997) K^+ channel regulation of signal propagation in dendrites of hippocampal pyramidal neurons. *Nature* **387,** 869–875
4. Cai, X., Liang, C. W., Muralidharan, S., Kao, J. P., Tang, C.-M., and Thompson, S. M. (2004) Unique roles of SK and Kv4.2 potassium channels in dendritic integration. *Neuron* **44,** 351–364

5. Tsaur, M.-L., Sheng, M., Lowenstein, D. H., Jan, Y. N., and Jan, L. Y. (1992) Differential expression of K^+ channel mRNAs in the rat brain and down-regulation in the hippocampus following seizures. *Neuron* **8,** 1055–1067
6. Castro, P. A., Cooper, E. C., Lowenstein, D. H., and Baraban, S. C. (2001) Hippocampal heterotopia lack functional Kv4.2 potassium channels in the methylazoxymethanol model of cortical malformations and epilepsy. *J. Neurosci.* **21,** 6626–6634
7. Bernard, C., Anderson, A., Becker, A., Poolos, N. P., Beck, H., and Johnston, D. (2004) Acquired dendritic channelopathy in temporal lobe epilepsy. *Science* **305,** 532–535
8. Monaghan, M. M., Menegola, M., Vacher, H., Rhodes, K. J., and Trimmer, J. S. (2008) Altered expression and localization of hippocampal A-type potassium channel subunits in the pilocarpine-induced model of temporal lobe epilepsy. *Neuroscience* **156,** 550–562
9. Singh, B., Ogiwara, I., Kaneda, M., Tokonami, N., Mazaki, E., Baba, K., Matsuda, K., Inoue, Y., and Yamakawa, K. (2006) A Kv4.2 truncation mutation in a patient with temporal lobe epilepsy. *Neurobiol. Dis.* **24,** 245–253
10. Norris, A. J., Foeger, N. C., and Nerbonne, J. M. (2010) Interdependent roles for accessory KChIP2, KChIP3, and KChIP4 subunits in the generation of Kv4-encoded IA channels in cortical pyramidal neurons. *J. Neurosci.* **30,** 13644–13655
11. Rhodes, K. J., Carroll, K. I., Sung, M. A., Doliveira, L. C., Monaghan, M. M., Burke, S. L., Strassle, B. W., Buchwalder, L., Menegola, M., Cao, J., An, W. F., and Trimmer, J. S. (2004) KChIPs and Kv4 α subunits as integral components of A-type potassium channels in mammalian brain. *J. Neurosci.* **24,** 7903–7915
12. Kuo, H. C., Cheng, C. F., Clark, R. B., Lin, J. J., Lin, J. L., Hoshijima, M., Nguyên-Trân, V. T., Gu, Y., Ikeda, Y., Chu, P. H., Ross, J., Giles, W. R., and Chien, K. R. (2001) A defect in the Kv channel-interacting protein 2 (KChIP2) gene leads to a complete loss of I(to) and confers susceptibility to ventricular tachycardia. *Cell* **107,** 801–813
13. Thomsen, M. B., Wang, C., Ozgen, N., Wang, H. G., Rosen, M. R., and Pitt, G. S. (2009) Accessory subunit KChIP2 modulates the cardiac L-type calcium current. *Circ. Res.* **104,** 1382–1389
14. He, X. P., Kotloski, R., Nef, S., Luikart, B. W., Parada, L. F., and McNamara, J. O. (2004) Conditional deletion of TrkB but not BDNF prevents epileptogenesis in the kindling model. *Neuron* **43,** 31–42
15. He, X. P., Pan, E., Sciarretta, C., Minichiello, L., and McNamara, J. O. (2010) Disruption of TrkB-mediated phospholipase Cγ signaling inhibits limbic epileptogenesis. *J. Neurosci.* **30,** 6188–6196
16. Racine, R. J. (1972) Modification of seizure activity by electrical stimulation. II. Motor seizure. *Electroencephalogr. Clin. Neurophysiol.* **32,** 281–294
17. Basarsky, T. A., Parpura, V., and Haydon, P. G. (1994) Hippocampal synaptogenesis in cell culture. Developmental time course of synapse formation, calcium influx, and synaptic protein distribution. *J. Neurosci.* **14,** 6402–6411
18. Bourdeau, M. L., Morin, F., Laurent, C. E., Azzi, M., and Lacaille, J.-C. (2007) Kv4.3-mediated A-type K^+ currents underlie rhythmic activity in hippocampal interneurons. *J. Neurosci.* **27,** 1942–1953
19. Barnwell, L. F., Lugo, J. N., Lee, W. L., Willis, S. E., Gertz, S. J., Hrachovy, R. A., and Anderson, A. E. (2009) Kv4.2 knockout mice demonstrate increased susceptibility to convulsant stimulation. *Epilepsia* **50,** 1741–1751
20. Patel, S. P., Parai, R., Parai, R., and Campbell, D. L. (2004) Regulation of Kv4.3 voltage-dependent gating kinetics by KChIP2 isoforms. *J. Physiol.* **557,** 19–41
21. Thiagarajan, T. C., Piedras-Renteria, E. S., and Tsien, R. W. (2002) α- and βCaMKII. Inverse regulation by neuronal activity and opposing effects on synaptic strength. *Neuron* **36,** 1103–1114
22. Turrigiano, G. (2012) Homeostatic synaptic plasticity. Local and global mechanisms for stabilizing neuronal function. *Cold Spring Harb. Perspect. Biol.* **4,** a005736
23. Andrásfalvy, B. K., Makara, J. K., Johnston, D., and Magee, J. C. (2008) Altered synaptic and non-synaptic properties of CA1 pyramidal neurons in Kv4.2 knockout mice. *J. Physiol.* **586,** 3881–3892
24. Magee, J. C., and Carruth, M. (1999) Dendritic voltage-gated ion channels regulate the action potential firing mode of hippocampal CA1 pyramidal neurons. *J. Neurophysiol.* **82,** 1895–1901
25. Chen, X., Yuan, L.-L., Zhao, C., Birnbaum, S. G., Frick, A., Jung, W. E., Schwarz, T. L., Sweatt, J. D., and Johnston, D. (2006) Deletion of Kv4.2 gene eliminates dendritic A-type K^+ current and enhances induction of long-term potentiation in hippocampal CA1 pyramidal neurons. *J. Neurosci.* **26,** 12143–12151
26. Chang, M. C., Park, J. M., Pelkey, K. A., Grabenstatter, H. L., Xu, D., Linden, D. J., Sutula, T. P., McBain, C. J., and Worley, P. F. (2010) Narp regulates homeostatic scaling of excitatory synapses on parvalbumin-expressing interneurons. *Nat. Neurosci.* **13,** 1090–1097
27. Hartman, K. N., Pal, S. K., Burrone, J., and Murthy, V. N. (2006) Activity-dependent regulation of inhibitory synaptic transmission in hippocampal neurons. *Nat. Neurosci.* **9,** 642–649
28. Kilman, V., van Rossum, M. C., and Turrigiano, G. G. (2002) Activity deprivation reduces miniature IPSC amplitude by decreasing the number of postsynaptic $GABA_A$ receptors clustered at neocortical synapses. *J. Neurosci.* **22,** 1328–1337
29. Lu, B. (2003) BDNF and activity-dependent synaptic modulation. *Learn. Mem.* **10,** 86–98
30. Maffei, A., Nelson, S. B., and Turrigiano, G. G. (2004) Selective reconfiguration of layer 4 visual cortical circuitry by visual deprivation. *Nat. Neurosci.* **7,** 1353–1359
31. Rutherford, L. C., DeWan, A., Lauer, H. M., and Turrigiano, G. G. (1997) Brain-derived neurotrophic factor mediates the activity-dependent regulation of inhibition in neocortical cultures. *J. Neurosci.* **17,** 4527–4535
32. Rutherford, L. C., Nelson, S. B., and Turrigiano, G. G. (1998) BDNF has opposite effects on the quantal amplitude of pyramidal neuron and interneuron excitatory synapses. *Neuron* **21,** 521–530
33. Cheng, H.-Y. M., Pitcher, G. M., Laviolette, S. R., Whishaw, I. Q., Tong, K. I., Kockeritz, L. K., Wada, T., Joza, N. A., Crackower, M., Goncalves, J., Sarosi, I., Woodgett, J. R., Oliveira-dos-Santos, A. J., Ikura, M., van der Kooy, D., Salter, M. W., and Penninger, J. M. (2002) DREAM is a critical transcriptional repressor for pain modulation. *Cell* **108,** 31–43
34. Lilliehook, C., Bozdagi, O., Yao, J., Gomez-Ramirez, M., Zaidi, N. F., Wasco, W., Gandy, S., Santucci, A. C., Haroutunian, V., Huntley, G. W., and Buxbaum, J. D. (2003) Altered Aβ formation and long-term potentiation in a calsenilin knock-out. *J. Neurosci.* **23,** 9097–9106
35. Buxbaum, J. D., Choi, E.-K., Luo, Y., Lilliehook, C., Crowley, A. C., Merriam, D. E., and Wasco, W. (1998) Calsenilin. A calcium-binding protein that interacts with the presenilins and regulates the levels of a presenilin fragment. *Nat. Med.* **4,** 1177–1181
36. Carrión, A. M., Link, W. A., Ledo, F., Mellström, B., and Naranjo, J. R. (1999) DREAM is a Ca^{2+}-regulated transcriptional repressor. *Nature* **398,** 80–84
37. Chang, B. S., and Lowenstein, D. H. (2003) Epilepsy. *N. Engl. J. Med.* **349,** 1257–1266
38. Patino, G. A., Brackenbury, W. J., Bao, Y., Lopez-Santiago, L. F., O'Malley, H. A., Chen, C., Calhoun, J. D., Lafrenière, R. G., Cossette, P., Rouleau, G. A., and Isom, L. L. (2011) Voltage-gated Na^+ channel β1B. A secreted cell adhesion molecule involved in human epilepsy. *J. Neurosci.* **31,** 14577–14591
39. Wallace, R. H., Wang, D. W., Singh, R., Scheffer, I. E., George, A. L., Jr., Phillips, H. A., Saar, K., Reis, A., Johnson, E. W., Sutherland, G. R., Berkovic, S. F., and Mulley, J. C. (1998) Febrile seizures and generalized epilepsy associated with a mutation in the Na^+-channel β1 subunit gene SCN1B. *Nat. Genet.* **19,** 366–370
40. Marionneau, C., Carrasquillo, Y., Norris, A. J., Townsend, R. R., Isom, L. L., Link, A. J., and Nerbonne, J. M. (2012) The sodium channel accessory subunit Navβ1 regulates neuronal excitability through modulation of repolarizing voltage-gated K^+ channels. *J. Neurosci.* **32,** 5716–5727
41. Burgess, D. L., Jones, J. M., Meisler, M. H., and Noebels, J. L. (1997) Mutation of the Ca^{2+} channel β subunit gene Cchb4 is associated with ataxia and seizures in the lethargic (lh) mouse. *Cell* **88,** 385–392
42. Barclay, J., Balaguero, N., Mione, M., Ackerman, S. L., Letts, V. A.,

Brodbeck, J., Canti, C., Meir, A., Page, K. M., Kusumi, K., Perez-Reyes, E., Lander, E. S., Frankel, W. N., Gardiner, R. M., Dolphin, A. C., and Rees, M. (2001) Ducky mouse phenotype of epilepsy and ataxia is associated with mutations in the Cacna2d2 gene and decreased calcium channel current in cerebellar Purkinje cells. *J. Neurosci.* **21,** 6095-6104

43. Bauer, C. S., Tran-Van-Minh, A., Kadurin, I., and Dolphin, A. C. (2010) A new look at calcium channel $\alpha 2\delta$ subunits. *Curr. Opin. Neurobiol.* **20,** 563–571
44. Surges, R., Thijs, R. D., Tan, H. L., and Sander, J. W. (2009) Sudden unexpected death in epilepsy. Risk factors and potential pathomechanisms. *Nat. Rev. Neurol.* **5,** 492–504